Kristina H. Haugaa, MD, PhD
Nina E. Hasselberg, MD
Thor Edvardsen, MD, PhD*
*Department of Cardiology
Oslo University Hospital
Rikshospitalet
N-0424 Oslo
Norway
E-mail: thor.edvardsen@medisin.uio.no

http://dx.doi.org/10.1016/j.jcmg.2014.04.029

Please note: This study was funded by South-Eastern Norway Regional Health Authority and The Research Council of Norway. Oslo University Hospital, Rikshospitalet has filed a patent application U.S. 61/306,678 regarding the method of mechanical dispersion. Drs. Haugaa and Edvardsen are the patent holders. Dr. Hasselberg has reported that she has no relationships relevant to the contents of this paper to disclose.

REFERENCES

1. Hasselberg NE, Edvardsen T, Petri H, et al. Risk prediction of ventricular arrhythmias and myocardial function in lamin A/C mutation positive subjects. Europace 2014;16:563–71.

2. Haugaa KH, Grenne BL, Eek CH, et al. Strain echocardiography improves risk prediction of ventricular arrhythmias after myocardial infarction. J Am Coll Cardiol Img 2013;6:841–50.

3. Haugaa KH, Goebel B, Dahlslett T, et al. Risk assessment of ventricular arrhythmias in patients with nonischemic dilated cardiomyopathy by strain echocardiography. J Am Soc Echocardiogr 2012;25:667–73.

4. Haugaa KH, Smedsrud MK, Steen T, et al. Mechanical dispersion assessed by myocardial strain in patients after myocardial infarction for risk prediction of ventricular arrhythmia. J Am Coll Cardiol Img 2010;3:247–56.

5. Haugaa KH, Amlie JP, Berge KE, Leren TP, Smiseth OA, Edvardsen T. Transmural differences in myocardial contraction in long-QT syndrome: mechanical consequences of ion channel dysfunction. Circulation 2010;122:1355–63.

Abnormal Myocardial Perfusion in Kawasaki Disease Convalescence

Kawasaki disease (KD) is a generalized systemic vasculitis, although the coronary artery system is typically involved. Coronary artery lesions (CAL) develop in 25% of children during the acute stage of KD and may lead to infarction, sudden death, or chronic coronary artery insufficiency (1). In about 50% of cases, complete, spontaneous resolution occurs within 1 year after onset (2).

The purpose of this study was to evaluate myocardial perfusion reserve with the use of perfusion cardiac magnetic resonance (CMR) in children with a previous history of KD and coronary involvement and correlate it with coronary morphologic abnormalities.

Fourteen asymptomatic patients with history of KD and coronary involvement (male patients, n = 8; mean age 10.2 ± 7.2 years) were prospectively examined with CMR using a 1.5-T magnetic resonance (MR) unit (Intera, Philips Healthcare, Best, the Netherlands). Electrocardiography-gated 2-dimensional steady-state free precession images were acquired for function assessment. Stress/rest first-pass perfusion was assessed using a turbo fast low-angle shot sequence (in-plane spatial resolution: 2.5 × 2.5 × 10.0 mm; 3 short-axis slices during intravenous contrast medium infusion (gadobutrol 0.1 mmol/kg body weight) after administration of 140 μg/kg/min adenosine for 4 min and at rest, with a 15-min interval. To assess fibrosis, late gadolinium enhancement (LGE) images were acquired 10 min after (inversion recovery turbo fast low-angle shot). A 3-dimensional steady-state free precession sequence with T_2 and fat saturation pre-pulses was used for MR angiography. Imaging was performed under anesthesia, if necessary, with continuous intravenous infusion of remifentanil and controlled ventilation.

Mean and segmental myocardial perfusion reserve index (MPRI), as defined by the ratio of stress to rest myocardial signal intensity relative upslope, were measured quantitatively (QMass MR 7.5, Medis, Leiden, the Netherlands). Left ventricular endocardial and epicardial boundaries of the left ventricle were automatically outlined and manually edited for through-plane motion on a 16-segment model, in time series of short-axis cine MR images. An abnormal coronary artery was defined according to criteria established by the Japanese Ministry of Health. A 5-SD threshold above the mean remote myocardial signal was used to study LGE images.

Comparisons of continuous variables with a normal distribution were performed using the independent-sample Student *t* test. Correlation analysis was assessed using Pearson correlation. The coefficient of variation was calculated to study the variability of the measurements. Data are expressed as mean ± SD unless otherwise specified. Values of $p < 0.05$ were considered statistically significant.

In 8 of 14 patients, CMR was performed under anesthesia. Persisting CAL were identified with MR angiography in 5 patients. Inducible perfusion defect by visual assessment was detected in 1 patient. LGE identified myocardial scar in 1 patient. Mean MPRI was significantly impaired in all patients, compared with historical pediatric control subjects (0.86 ± 0.256 vs. 2.46 ± 0.3, $p < 0.001$, 1 sample Student *t* test) (3). No significant difference in mean MPRI was identified between patients with regressed CAL (9 of 14) and persistent CAL (5 of 14) (1.0 ± 0.3 vs. 0.79 ± 0.225; $p = 0.31$). In patients with persisting CAL, no differences in MPRI were demonstrated between segments subtended by arteries with regressed and persistent CAL. Patients' clinical and CMR characteristics are presented in **Table 1**.

Previous histologic studies in the acute and chronic phase of KD have confirmed inflammatory cell

TABLE 1 Clinical and CMR Characteristics of KD Patients (N = 14)

Age at CMR examination, yrs	10.2 ± 7.2
Male	8/14 (57)
Age at KD onset, yrs	5.0 ± 3.5
Interval from acute event, yrs	4.9 ± 5.6
Treatment	
IVIG	14/14 (100)
Aspirin	14/14 (100)
Steroids	0/0 (0)
Exam under anesthesia	8/14
Coronary artery status by MRA	
Transient CAL	9/14 (64)
Persistent CAL	5/14 (36)
Dilation of RCA origin/dilation of LAD-LCX bifurcation mm	3/4
Dilation of LMCA, mm	4
Dilation of LAD origin, mm	4
Dilation of LM/LAD, mm	4
Giant aneurysm of LMCA/LAD aneurysm, mm	17/4
Function	
LVEF, %	60.0 ± 4.7
Normal	67.0 ± 5.0
LV EDVI, ml/m^2	73.0 ± 22.4
Normal	90.0 ± 11.0
LV ESV, ml/m^2	29.0 ± 10.1
Normal	30.0 ± 7.0
Myocardial perfusion	
Inducible visual defect	1/14
Basal to apical lateral subendocardial defect, related to LMCA giant aneurysm	
Mean MPRI, all patients	0.86 ± 0.256
Mean MPRI, transient CAL	1.0 ± 0.30
Mean MPRI, persistent CAL	0.79 ± 0.225
LGE+	1/14
Basal inferior subendocardial scar	

Values are mean ± SD, n/N (%), n/N, or n.

+ = positive; CAL = coronary artery lesion; CMR = cardiac magnetic resonance; EDVI = end-diastolic volume indexed; ESV = end-systolic function; IVIG = intravenous immunoglobulin; KD = Kawasaki disease; LAD = left anterior descending artery; LCX = left circumflex artery; LGE = late gadolinium enhancement; LMCA = left main coronary artery; LVEF = left ventricular ejection fraction; MRA = magnetic resonance angiography; MPRI = myocardial perfusion reserve index; RCA = right coronary artery.

infiltration of the arterial wall, with subsequent reparative elastic fibers replacement by fibrous tissue and chronic myofibroblastic intimal proliferation (4). A limited number of studies with nuclear medicine tracers in KD patients identified reduced hyperemic flow and flow reserve, despite resolution of epicardial vessel disease, as indicative of functional microvascular abnormalities (5).

In our study, we demonstrated with the use of CMR that MPRI was markedly decreased in all myocardial segments regardless of the epicardial disease status. These findings are in agreement with previous studies, suggesting that microvascular dysfunction is a substantial feature of the underlying diseased myocardium.

Only quantitative perfusion analysis was able to detect the abnormalities due to the lack of regional differences in perfusion. Quantitative CMR perfusion imaging influences substantially the appreciation of myocardial perfusion pattern in KD and provides further insight into its pathophysiological substrate.

The limitations of the study were the small number of patients and the lack of a pediatric normal reference group, due to the ethical obstacles in applying a stress exam in a healthy pediatric population.

In conclusion, quantitative perfusion CMR identifies abnormal perfusion reserve in KD convalescent patients irrespective of the coronary artery status, which is suggestive of significant coronary microvascular dysfunction. The clinical implications of these findings need further assessment.

Konstantinos Bratis, MD
Amedeo Chiribiri, MD, PhD
Tarique Hussain, MD, PhD
Thomas Krasemann, MD
Marcus Henningsson, MD, PhD
Alkystis Phinikaridou, MD, PhD
Sophie Mavrogeni, MD
Rene Botnar, MD, PhD
Eike Nagel, MD, PhD
Reza Razavi, MD, PhD
Gerald Greil, MD, PhD*

*Department of Cardiovascular Imaging Sciences
The Rayne Institute
St. Thomas' Hospital
King's College London
4th Floor, Lambeth Wing
Westminster Bridge Road
SE1 7EH, London
United Kingdom
E-mail: gerald.greil@kcl.ac.uk

http://dx.doi.org/10.1016/j.jcmg.2014.05.017

Please note: This study is supported by funding from the Department of Health through the National Institute for Health Research comprehensive Biomedical Research Centre award to Guy's and St. Thomas' National Health Service Foundation Trust in partnership with King's College London and King's College Hospital National Health Service Foundation Trust. The Division of Imaging Sciences also receives support as the Centre of Excellence in Medical Engineering (funded by the Wellcome Trust and the Engineering and Physical Sciences Research Council; grant #WT 088641/Z/09/Z) as well as from a British Heart Foundation Centre of Excellence award (#RE/08/03). Dr. Nagel has received significant grant support from Bayer Schering Pharma and Philips Healthcare. Dr. Chiribiri has received grant support from Philips Healthcare. All other authors have reported that they have no relationships relevant to the contents of this paper to disclose. Nathaniel Reicheck, MD, served as Guest Editor for this paper.

REFERENCES

1. Sundel RP, Newburger JW. Kawasaki disease and its cardiac sequelae. Hosp Pract (Off Ed) 1993;28:51–4, 57–60, 64–6.

2. Greil GF, Manning WJ. Treatment of Kawasaki disease. N Engl J Med 2007; 356:2747–8, author reply 2748.

3. Madriago EWR, Jerosch-Herold M, Diggs SB, et al. Impaired adenosine-induced myocardial perfusion in children with mild/moderate aortic stenosis

using quantitative magnetic resonance imaging. J Cardiovasc Magn Reson 2011;13 Suppl 1:P209.

4. Rowley AH, Orenstein JM. Clinical implications of a new model of Kawasaki disease arteriopathy. Pediatr Cardiol 2013;34:1290–1.

5. Hauser M, Bengel F, Kuehn A, et al. Myocardial blood flow and coronary flow reserve in children with "normal" epicardial coronary arteries after the onset of Kawasaki disease assessed by positron emission tomography. Pediatr Cardiol 2004;25:108–12.

Noninvasive Evaluation of Bone-Forming Activity Within the Calcified Atherosclerotic Lesions by Tc 99m HMDP Scintigraphy

The process of active calcium deposition as demonstrated by radiolabeled fluoride uptake has been recently proposed to be associated with high-risk plaques (1). Similarly, the computed tomography (CT)-verified spotty calcification is associated with the plaques that have resulted in recent acute coronary events (2). However, although coronary artery calcium score has been shown to positively correlate with cardiovascular disease risk, extensive vascular calcification, probably representing a burnt-out disease, may be more prominently associated with stable plaques (3). Because vascular calcification does not occur in a degenerative and passive process of calcium deposition, and may represent an active phenotypic change associated with bone mineralization (4), bone-forming activity within the atherosclerotic plaques rather than calcium volume and/or calcium density scores might be a better marker for predicting future cardiovascular events. Indeed, serum levels of alkaline phosphatase, a marker of osteoblastic activity, have been associated with all-cause or cardiovascular mortality among survivors of myocardial infarction and in a general population (5). Similar to the fluoride imaging of the active process of calcification, we measured the osteoblastic activity within the carotid atherosclerotic plaques by using a technetium Tc 99m hydroxy-methylene-diphosphonate (^{99m}Tc-HMDP) scintigraphy.

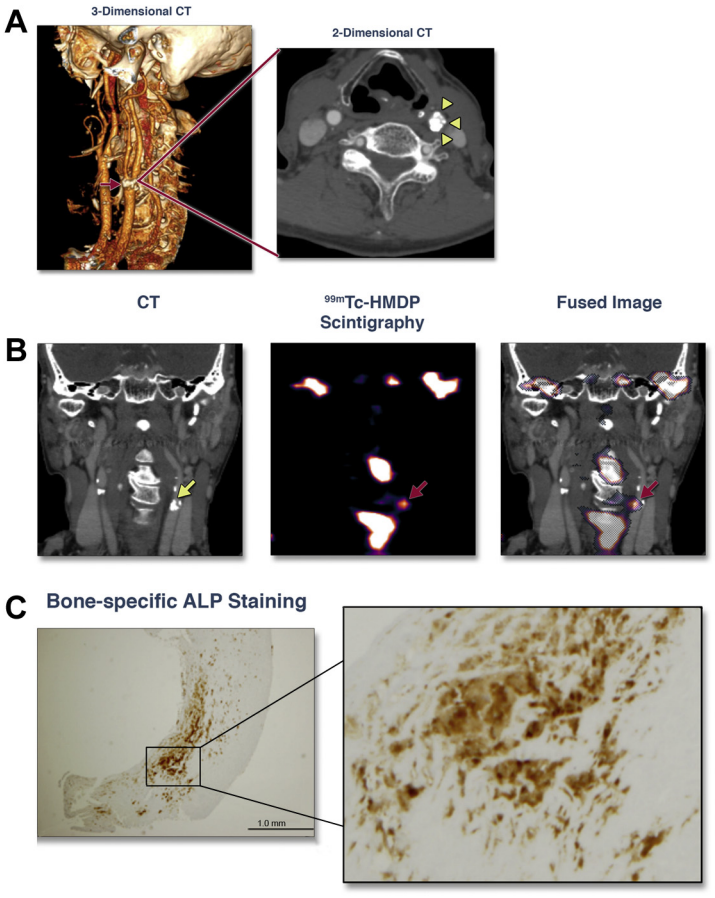

FIGURE 1 Bone-Forming Activity Within the Calcified Atherosclerotic Lesions by ^{99m}Tc-HMDP Scintigraphy

(A) Three- and 2-dimensional images of multislice computed tomography (CT) angiography demonstrated a calcified carotid atherosclerosis **(left: red arrow; right: yellow arrowheads). (B)** An intense uptake of technetium Tc 99m hydroxy-methylene-diphosphonate (^{99m}Tc-HMDP) was observed (^{99m}Tc-HMDP scintigraphy and fused images, **red arrows**) in the calcified carotid atherosclerosis (CT image, **yellow arrow**). **(C)** Immunohistochemical analysis revealed that expression levels of bone-specific alkaline phosphatase (ALP) were increased in the calcified lesion of atherosclerosis. Inset showed magnification of the marked area **(square)**.

A 72-year-old man with a history of hyperuricemia, dyslipidemia, and hypertension had a bruit in his left neck. Although he had no symptoms associated with brain ischemia, carotid artery ultrasonography and CT angiography showed the calcified atherosclerotic lesions of the left internal carotid artery (Figure 1A). The peak systolic velocity in the left internal carotid artery was 255.8 cm/s (normal range <200 cm/s) in Doppler carotid artery ultrasonography, and a left post-bulbar internal carotid artery stenosis was 85% in a diagnostic angiography. In coregistration of enhanced CT and bone scintigraphy, an intense accumulation of ^{99m}Tc-HMDP was observed within the calcified carotid atherosclerotic lesions (Figure 1B). There was no measurable accumulation of ^{99m}Tc-HMDP in other atherosclerotic lesions without vascular calcification. Based on the NASCET (North American Symptomatic Carotid Endarterectomy Trial) guidelines, he was a very high-risk patient for cerebrovascular disease, and the carotid endarterectomy was performed. Immunohistochemical analysis revealed that bone-specific alkaline phosphatase was abundantly expressed in the excised calcified lesions of atherosclerosis (Figure 1C).

Because ^{99m}Tc-HMDP has a strong affinity for hydroxyapatite crystals in the mineral phase of bone, especially sites of new bone formation, the present report suggests that bone scintigraphy with ^{99m}Tc-HMDP might be a feasible and useful method to